Peer-reviewed version available at *Catalysts* **2018**, *8*, 264; doi:10.3390/catal8070264

Acid-Base Bifunctional Hf Nanohybrids-Enabled High Selectivity in Catalytic Conversion of Ethyl Levulinate to γ-Valerolactone

Weibo Wu,[1] Yan Li,[1] Hu Li,[*,1] Wenfeng Zhao,[1] Song Yang[*,1]

[1] *State Key Laboratory Breeding Base of Green Pesticide & Agricultural Bioengineering, Key Laboratory of Green Pesticide & Agricultural Bioengineering, Ministry of Education, State-Local Joint Laboratory for Comprehensive Utilization of Biomass, Center for Research & Development of Fine Chemicals, Guizhou University, Guiyang, Guizhou 550025, China; weibo_wu@foxmail.com (W.W.); 15761698544@163.com (Y.L.); hli13@gzu.edu.cn (H.L.); 18275623845@163.com (W.Z.); jhzx.msm@gmail.com (S.Y.)*

* Correspondence:

jhzx.msm@gmail.com (S.Y.); hli13@gzu.edu.cn (H.L.); Tel.: +86-851-8829-2171

Peer-reviewed version available at Catalysts 2018, 8, 264; doi:10.3390/catal8070264

Abstract

Catalytic upgrading of bio-based platform molecules is one of promising approaches for biomass valorization. However, most solid catalysts are thermally and/or chemically unstable and difficult to prepare. In this study, a stable organic phosphonate-hafnium solid catalyst (PPOA-Hf) was synthesized, and acid-base bifunctional sites were found to play a cooperative role in the cascade transfer hydrogenation and cyclization of ethyl levulinate (EL) to γ-valerolactone (GVL). Under relatively mild reaction conditions of 160 ºC for 6 h, EL was completely converted to GVL in a good yield of 85%. The apparent activation energy was calculated to be 53 kJ/mol, which was lower than other solid catalysts for the same reaction. In addition, the PPOA-Hf solid catalyst did not significantly decrease its activity after five recycles, and no evident leaching of Hf was observed, indicating its high stability and potential practical application.

Keywords

Heterogeneous catalysis; transfer hydrogenation; biomass conversion; biofuels; catalytic materials

1. Introduction

Nowadays, with the continuous development of human society, the demand for energy and fine chemicals is increasing [1]. However, the use and gradual depletion of fossil resource needs people to face and solve a series of problems, such as environmental pollution, greenhouse effect, and energy crisis [2]. The development of renewable energy is thus highly demanded, where biomass source is the only sustainable carbon feedstock, showing great potential for practical applications [3]. Lignocellulose is abundant in nature, which has been demonstrated to be capable of being efficiently converted to a series of high valuable chemicals and biofuels through chemo-catalytic reactions coupled with well-designed processes [4,5].

As one of biomass-derived versatile platform molecules, γ-valerolactone (GVL) can be used as a green solvent for biomass conversion and organic transformations [6]. In addition, it is able to be employed for producing biofuels and fuel additives (e.g., 2-methyltetrahydrofuran) [7] and as a key intermediate in the synthesis of fine chemicals (e.g., pentenoic acid, α-methylene-γ-valerolactone (MeGVL)), as shown in Scheme 1 [8,9]. Typically, GVL can be prepared from lignocellulose following sequential catalytic pathways involving different reactions such as hydrolysis, isomerization, dehydration, etherification, esterification, hydrogenation and lactonization [10-16]. Amongst these conversion processes, cascade hydrogenation and cyclization are deemed as the key step for catalytic upgrading of levulinic acid and its esters to GVL in recent several years [17-18].

Preprints (www.preprints.org) | NOT PEER-REVIEWED | Posted: 28 May 2018 doi:10.20944/preprints201805.0402.v1

Peer-reviewed version available at Catalysts 2018, 8, 264; doi:10.3390/catal8070264

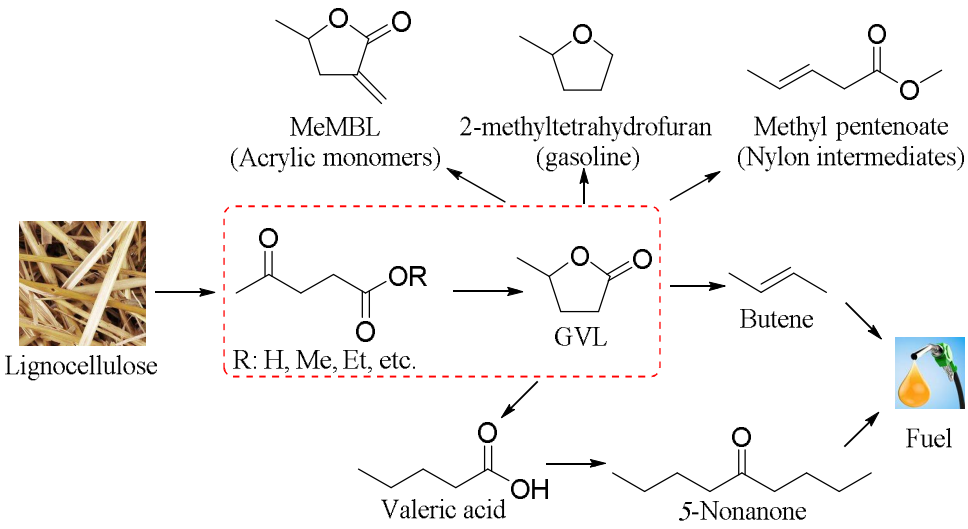

Scheme 1. Synthesis and application of GVL

Catalytic transfer hydrogenation (CTH) is widely used in the reduction of carbonyl compounds, where H_2 gas is replaced by other liquid molecules (e.g., formic acid and alcohols) as hydrogen-donors [19-21]. It is worth noting that there is a certain requirement for the quality of the used reactor and the catalyst stability to tolerate acidic reaction conditions [22,23]. In this regard, alcohols seem to be a better candidate for CTH. As one of well-known examples, Zr-incorporated zeolites with appropriate Lewis acidity have been reported to be able to efficiently catalyze CTH of biomass-derived carboxides, alike to Meerwein-Ponndorf-Verley (MPV) reduction [24-26].

In the past decade, Zr-based catalysts have been reported to be efficient for CTH of levulinic acid and its esters to GVL, and their reactivity is highly dependent on the catalyst compositions. For instance, ZrO_2 [27,28], $Zr(OH)_4$ [29], $ZrFeO_x$ [30], Al-Zr [31], Zr-B [32], and $ZrOCl_2$ [33] need relatively harsh conditions (ca. 200 ºC or > 6 h) to achieve moderate yields of GVL. The stability and catalytic performance can be improved by incorporation of Zr species into solid supports like SBA-15, while it generally involves complicated preparation procedures and relatively high production

cost due to the use of template agents [34]. Therefore, it is necessary to overcome these shortcomings by improving the catalyst stability with facile preparation method.

Organic phosphonates as ligands combined with metal ions can fast take place under liquid-phase conditions to afford corresponding inorganic-organic metal phosphonates with enhanced chemical and thermal stability [35-41]. Through the coordination of metal ions with organic phosphoric acid, additional micro- and mesopores are introduced into the resulting catalysts, thus greatly rendering increased specific surface areas [42,43], and the catalyst functionalities can be simply tuned by changing the organic ligand or preparation method [44]. In the present study, a stable inorganic-organic metal phosphonate catalyst (PPOA-Hf) was prepared from phenylphosphonic acid (PPOA) and hafnium (Hf, in the same group as Zr on the periodic table) chloride by using a simple assembly method. This acid-base bifunctional solid catalyst was able to efficiently promote EL being converted to GVL under mild reaction conditions, and systematic studies were thereby conducted.

2. Materials and experiments

2.1. Materials

Hafnium (IV) chloride ($HfCl_4$; 99%) and phenylphosphonic acid (PPOA; 98%) were purchased from Adamas Reagent Co., Ltd. Ethyl levulinate (EL; 98%) were purchased from Alfa Aesar (China) Chemicals Co., Ltd. Naphthalene (99%), γ-valerolactone (GVL; 98%), 2-propanol (99.5%) and other reagents were purchased from Beijing Innochem Technology Co., Ltd., and directly used for the study unless otherwise noted.

2.2. Catalyst Preparation

Halfnium phenylphosphonates (PPOA-Hf-*x*, *x* denotes the used molar ratio of PPOA to Hf) were prepared from PPOA and $HfCl_4$ with corresponding PPOA/Hf ratios. In a typical procedure for the synthesis of PPOA-Hf-1:1.5, 20 mmol PPOA (0.3162 g) was initially dissolved into 60 mL *N,N*-dimethylformamide (DMF) in a Teflon-lined tube, followed by dropwise addition of 30 mmol $HfCl_4$ (0.9609 g) under vigorously stirring conditions. After stirring for 20 min, the hydrothermal reactor was sealed and placed into an oven heating at 120 ºC for 24 h. Upon completion, the solid precipitates were separated out from the liquid mixture by filtration, successively washed with DMF (100 mL), ethanol (100 mL), and methanol (100 mL) for 2-3 times, and finally dried at 45 ºC overnight to give the catalyst PPOA-Hf-1:1.5.

2.3. Catalyst Characterization Techniques

BET (Brunauer-Emmett-Teller) surface areas of the porous materials were determined from nitrogen physisorption measurements at liquid nitrogen temperature on a Micromeritics ASAP 2460 instrument. FT-IR (Fourier transform infrared spectrometer) spectra were measured by Thermo Fisher Nicolet iS50 spectrometer in wavenumber range of 400-4000 cm^{-1}. The Lewis and Brønsted acid sites of PPOA-Hf was determined by vacuum adsorption surface reaction infrared in situ characterization analysis system (Dalian Institute of Chemical Physics, Chinese Academy of Sciences) with Thermo Fisher Nicolet iS50 AEM in wavenumber range of 1400-1600 cm^{-1}. Content of Hf and P species in reaction system were determined by inductively coupled plasma-optical emission spectrometer (ICP-OES) on a PerkinElmer Optima 5300 DV. STEM (scanning transmission electron microscopy) and TEM (Transmission electron microscope) test was measured by JEOL 2100 TEM/STEM. Thermogravimetry (TG) analysis was carried out by a NETZSCH STA 449 F3 Jupiter thermal gravimetric analyzer. The acidity and basicity of catalysts were measured by NH_3-TPD and CO_2-TPD (temperature programmed desorption) using a Micromeritics AutoChem 2920 chemisorption analyzer.

XPS (X-ray photoelectron spectroscopy) measurements were recorded using a Physical Electronics Quantum 2000 Scanning ESCA Microprobe (Physical Electronics Inc., PHI, MN) equipped with a monochromatic Al Kα anode. The data of XRD (X-ray diffraction) of the powder samples were obtained by using a Rigaku International D/max-TTR III X-ray powder diffractometer with Cu Kα radiation and 2θ scanned from 5° to 80°.

2.4. Catalytic Activity Measurements

The reactions for conversion of EL to GVL were all carried out in a 10 mL Teflon-lined autoclave heated by an oil bath. In a general procedure, 1 mmol EL (144 mg), 72 mg catalyst and 5 mL 2-propanol were added into the Teflon-lined reactor. The sealed reaction kettle was then put into the oil bath at a prefixed temperature, and the reaction time was accordingly recorded. After reaction, the solid catalyst was removed by centrifugation, and the liquid mixture passed through filter membrane (0.22 μm) prior to GC and GC-MS analysis.

2.5. Product Analysis

Liquid products were identified by Agilent 6890N GC-MS with 5973MS mass spectrometer. For quantitative analysis of EL and GVL, an Agilent GC7890B equipped with a HP-5 19091J-413 column (30 m × 0.32 mm × 0.25 mm) and a FID detector was used Internal standard method was adopted for quantitative calculation based on standard curves ($R^2 > 0.99$) of EL and GVL, and naphthalene was used as the internal standard substance. Substrate conversion (X, %) and product yield (Y, %) were calculated using below equations:

X (%) = [1 - (mole of substrate after reaction) / (mole of initial substrate)] × 100% **(1)**

Y (%) = (mole of obtained product)/ (mole of initial substrate) ×100% **(2)**

2.6. Catalyst Recycling

Peer-reviewed version available at Catalysts 2018, 8, 264; doi:10.3390/catal8070264

After each cycle of reactions, the catalyst was separated by centrifugation from the reaction mixture, successively washed with 10 mL DMF, ethanol and methanol, and then dried at 45 ºC for 12 h. The resulting solid catalyst was directly used for the next run.

3. Results and discussions

3.1. Catalyst Characterization

Prior to conducting catalytic reactions, the PPOA-Hf catalyst was characterized by BET, STEM, TEM, TG, XRD and PY-IR. PPOA-Hf-1:1.5 was examined to be mesoporous (average pore diameter 3.4 nm) with surface area of 215 m^3/g and pore volume of 0.16 cm^3/g by N_2 adsorption-desorption isotherms (Fig. 1A). From PY-IR spectrum in Fig. 1B, it can be seen a peak at 1450 cm^{-1}, which is indicative of Lewis acid sites in PPOA-Hf. Moreover, there are small peaks at 1490 and 1520 cm^{-1}, showing the presence of weak Brønsted acid sites in PPOA-Hf. TG analysis was conducted to study the thermal stability of PPOA-Hf (Fig. 1C). It is interesting to note that less than 10% catalyst weight was lost till 400 ºC and increased weight loss was observed when reaching 550 ºC. This result indicates that the PPOA-Hf catalyst is thermally stable and can be a good candidate for chemical reaction under thermal conditions. XRD analysis shows that PPOA-Hf does not have high crystalline (Fig. 1D), with some wide bands belonging to tetragonal (t) and monoclinic (m) phases, while the peak at $2\theta = 6^{\circ}$ is possibly resulted from the interlayer clearance of the phosphate [45].

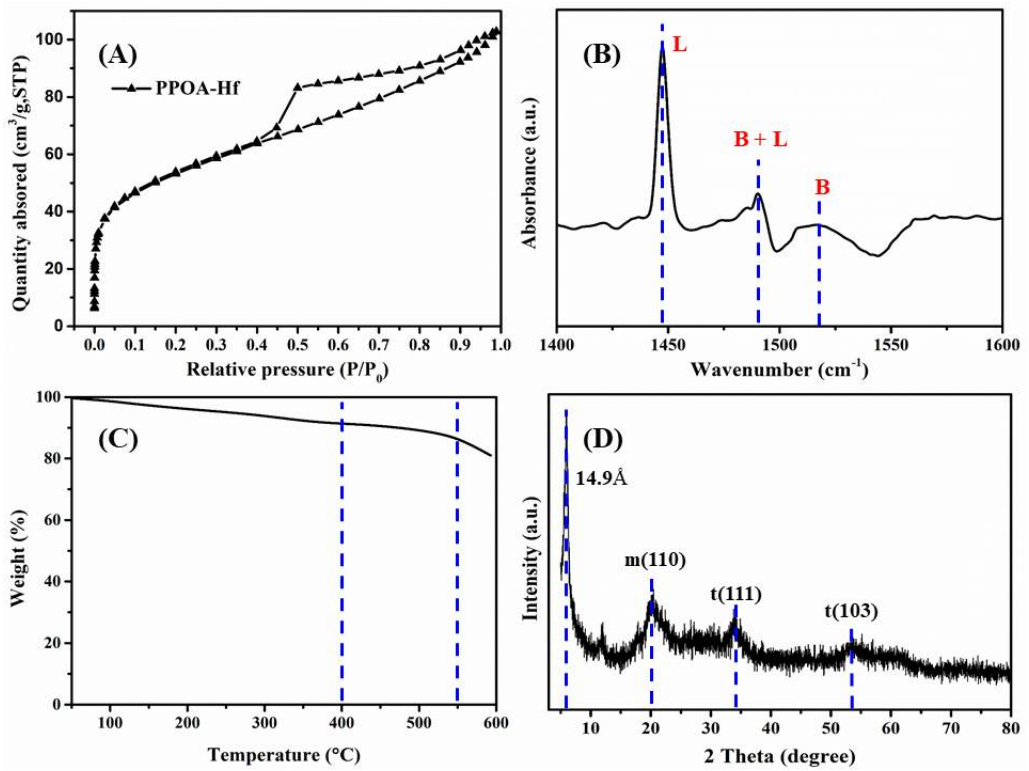

Fig. 1 N_2 adsorption-desorption isotherms (A), PY-IR spectrum (B), TG curve (C) and XRD pattern (D) of PPOA-Hf-1:1.5; L = Lewis acid; B = Brønsted acid.

TEM images further confirm that PPOA-Hf-1:1.5 (Fig. 2A) is noncrystalline as compared with HfO_2 (Fig. 2B), and the detected lamellar structure is consistent with the result (2θ = 6º) clarified by XRD (Fig. 1A). Gratifyingly, the particle size of PPOA-Hf-1:1.5 seems to be smaller than that of HfO_2 (Fig. 2), due to its amorphous structure. Further, STEM elemental mappings indicate the even and well-connected combination of organic ligand and Hf (Fig. 3).

Preprints (www.preprints.org) | NOT PEER-REVIEWED | Posted: 28 May 2018 doi:10.20944/preprints201805.0402.v1

Peer-reviewed version available at Catalysts 2018, 8, 264; doi:10.3390/catal8070264

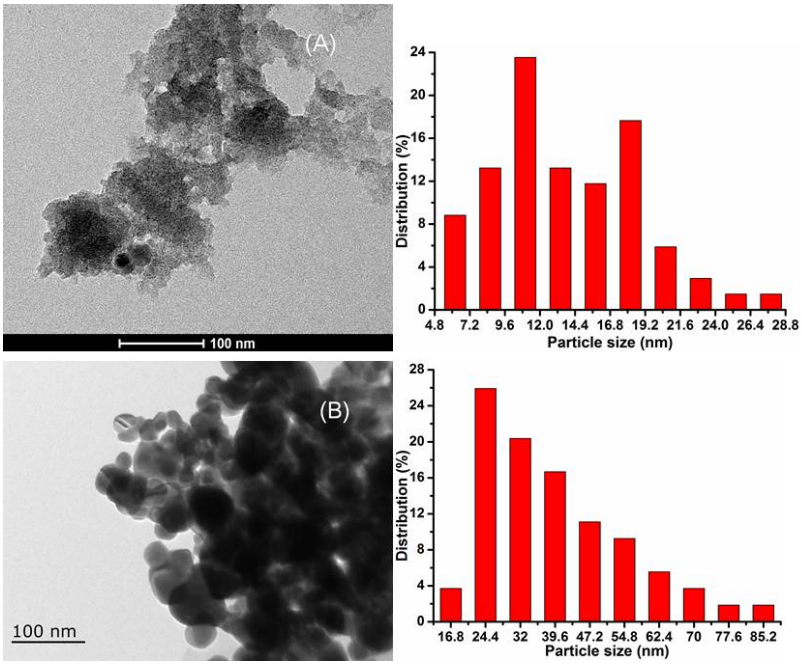

Fig. 2 TEM images and particle size distribution of (A) PPOA-Hf-1:1.5 and (B) HfO_2

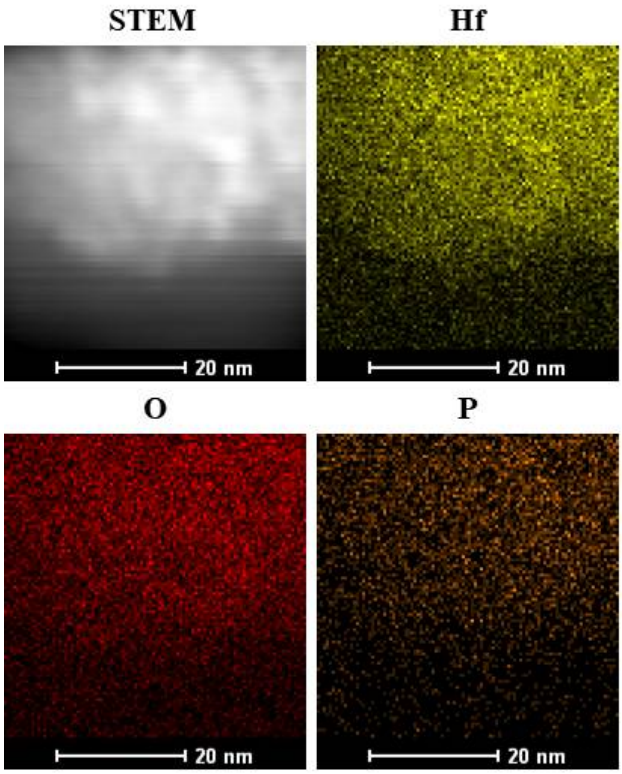

Fig. 3 STEM image and elemental mappings of PPOA-Hf-1:1.5

The base and acid properties of PPOA-Hf-*x* catalysts in different molar ratios of PPOA/Hf were determined by CO_2-TPD and NH_3-TPD, respectively. As shown in Fig. 4, it can be clearly observed that PPOA-Hf is an acid-base bifunctional catalyst, and the contents of acid and base sites increase with the increase of Hf relative to PPOA. In addition, the amount of acid-base sites remained nearly unchanged after recycling for five times, indicating that PPOA-Hf catalyst was stable and reusable.

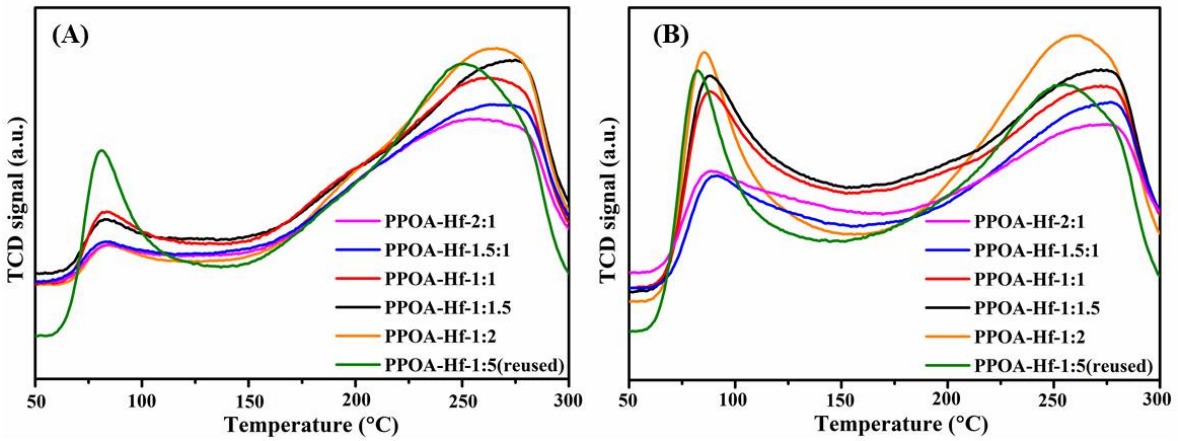

Fig. 4 CO_2-TPD (A) and NH_3-TPD (B) patterns of PPOA-Hf-*x* with different PPOA/Hf molar ratios

The strength of acid and base sites was investigated by XPS analysis, and the results are provided in Fig. 5. Typically, low and high binding energy of O 1s and Hf 4f are indicative of high strength of both base and acid sites [46]. It is not difficult to see that the strength of acidic and basic sites in the PPOA-Hf-*x* catalysts is negatively correlated with the increase of PPOA/Hf ratio (Fig. 5). In this respect, both content and strength of acid-base sites in PPOA-Hf-*x* can be controlled by adjusting the molar ratio of PPOA/Hf.

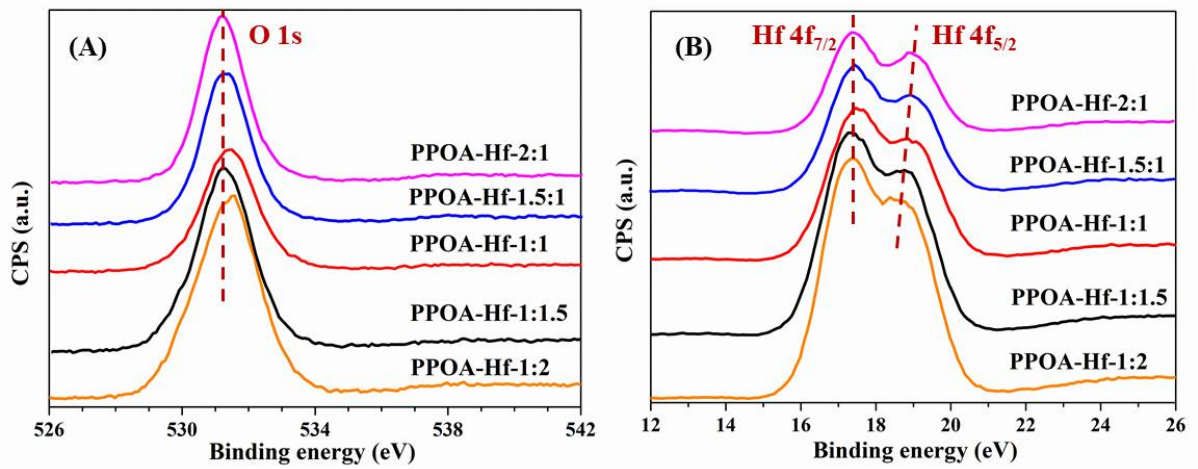

Fig. 5 XPS spectra of (A) O 1s and (B) Hf 4f in PPOA-Hf-*x* with different PPOA/Hf molar ratios

To clearly elucidate the functional structure of PPOA-Hf-*x*, FT-IR analysis was finally conducted, and the spectra are shown in Fig.6. In area A, the peak of Hf-O (500-800 cm^{-1}) is clearly visible in the spark line of HfO_2. On the other hand, the peaks at 600 cm^{-1} (corresponding to aromatic ring) and 700 cm^{-1} (out-of-plane bending vibration of C-H bond) decrease sharply with the increase of Hf content, implying the tight combination of hafnium and organic ligand. Interestingly, with the combination of PPOA and Hf, the position of the O-H (2400-3200cm^{-1}) bond and Ph-H (1900-2300 cm^{-1}) shifted to 3200-3700 cm^{1} and 3000-3100 cm^{1}. In addition, the characteristic peaks of P-O (1000 cm^{-1}), C-P (1150-1200 cm^{-1}) and C=C (1400-1700 cm^{-1}) are all present, indicating the well connection of organic ligand and Hf and the possible origin of acid and base sites (e.g., Brønsted acid sites: -OH; Lewis acid-base sites: -Hf-O-P-).

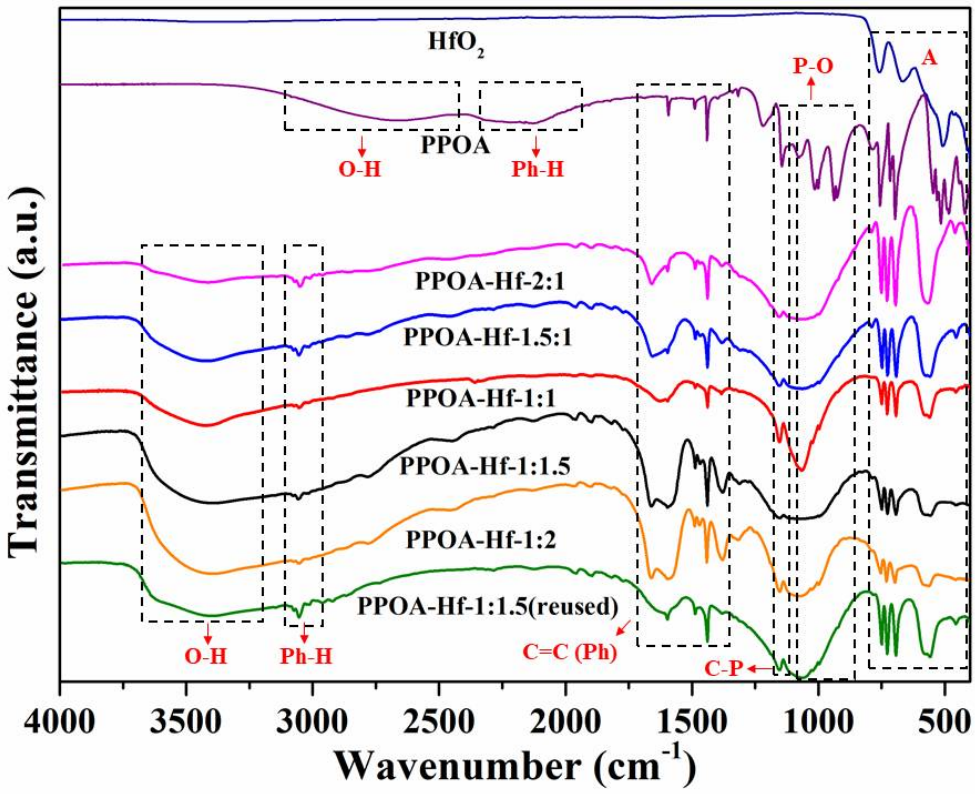

Fig. 6 FT-IR patterns of PPOA-Hf–*x* with different PPOA/Hf molar ratios

3.2. Catalytic Performance of PPOA-Hf-x

The catalytic activity of *PPOA-Hf-x* with different PPOA/Hf molar ratios in CTH reaction of EL to GVL was investigated at first, and the results are shown in Fig.7. It is obvious to observe that as the ratio of PPOA/Hf ranges from 2:1 to 1:1.5, the conversion rate of EL and the yield of GVL increase from 72% and 55% to 100% and 85% respectively. This tendency is approximately consistent with the content and strength of acid-base sites (Fig. 4 and Fig. 5B). But further rise of the PPOA/Hf ratio to 1:2 did not increase the yield of GVL, showing the acidity and basicity of PPOA-Hf-1:1.5 is appropriate for GVL synthesis from EL. Therefore, PPOA-Hf-1:1.5 is considered to be the optimal catalyst for subsequent studies.

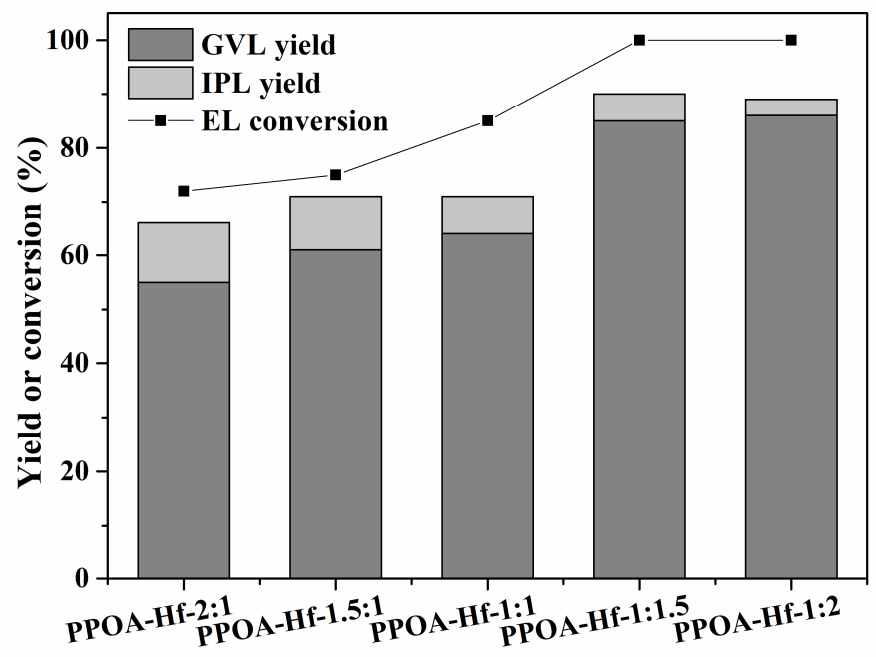

Fig. 7 Catalytic results of PPOA-Hf-*x* with different PPOA-Hf molar ratios in conversion of EL to GVL; Reaction conditions: EL: 1 mmol, catalyst: 72 mg, 2-propanol: 5 mL, T: 160 ºC, t: 6 h.

3.3. Effect of Reaction Time and Temperature

Reaction temperature and time are important parameters for reactivity control in the chemical reactions. The effect of reaction temperature (120-180 ºC) on the conversion of EL to GVL over PPOA-Hf-1:1.5 in 6 h was studied, and the results are shown in Fig. 8. Relatively high yield of GVL (ca. 85%) can be obtained in 6 h at 160 ºC and 4 h at 180 ºC respectively. Isopropyl levulinate (IPL) was detected as the dominant byproduct, which reduces the selectivity of GVL. From an economic point of view, the optimal reaction conditions should be 160 ºC and 6 h.

Preprints (www.preprints.org) | NOT PEER-REVIEWED | Posted: 28 May 2018 doi:10.20944/preprints201805.0402.v1

Peer-reviewed version available at Catalysts 2018, 8, 264; doi:10.3390/catal8070264

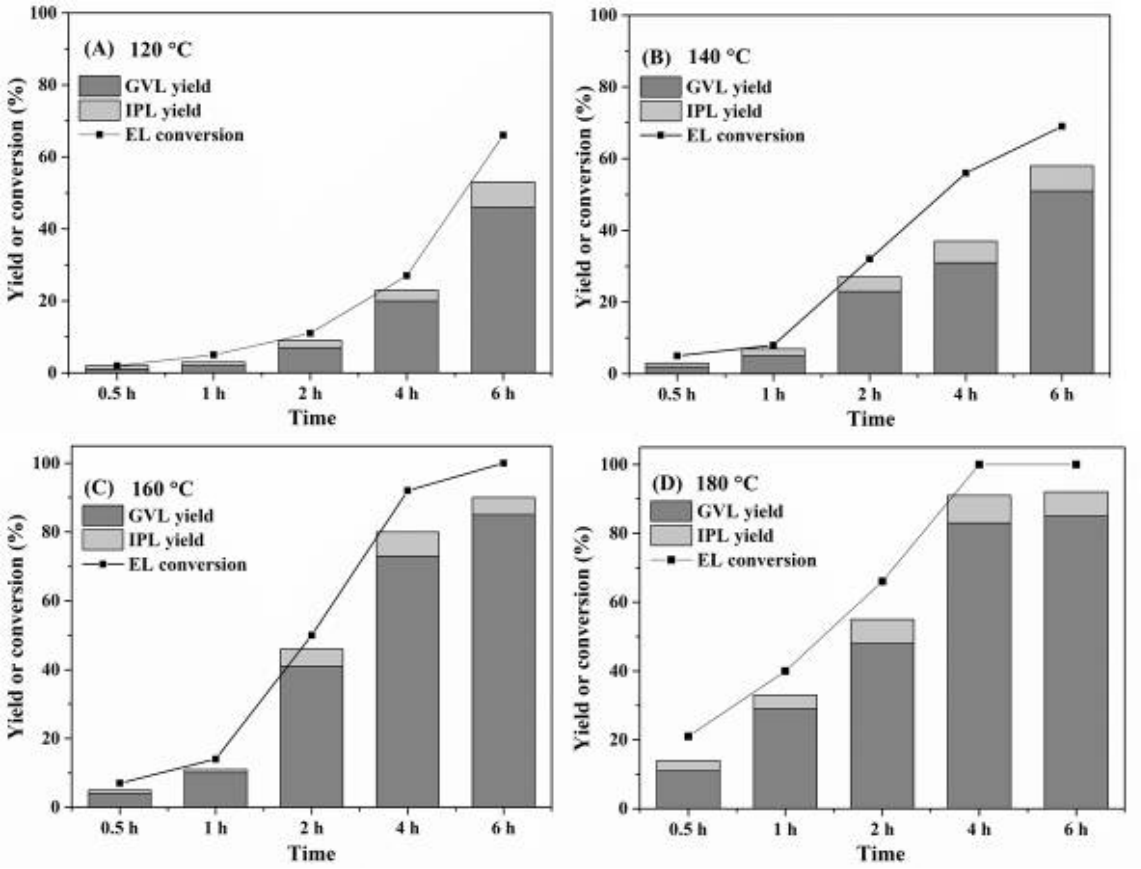

Fig. 8 Effect of reaction temperature (120-180 ℃) and time on the conversion of EL to GVL; Reaction conditions: EL: 1 mmol, PPOA-Hf-1:1.5: 72 mg, 2-propanol: 5 mL.

In addition, the kinetics of EL-to-GVL conversion was studied by assumption of pseud 1st order reaction, where four reaction temperatures of 120 ℃ (393 K), 140 ℃ (413 K), 160 ℃ (433 K) and 180 ℃ (453 K) were selected. Well-fitted linear curves by plotting -ln(1-*X*) (*X* = FUR conversion) with time were obtained for different reaction temperatures, as shown in Fig. 9A. The apparent activation energy (E_a) was calculated to be 53kJ/mol according to the Arrhenius equation, after the obtained reaction rate constant (ln*k*) being plotted with temperature (1/T; Fig. 9B). This value is much lower than other previously reported catalytic systems, such as Shvo-Ru (69 kJ/mol) [47], Ru tris(m-sulfonatophenyl)phosphine (61 kJ/mol) [48], and Ti-Beta (69 kJ/mol) [49],

indicating that PPOA-Hf-1:1.5 is an more effective and promising solid catalyst for catalytic conversion of EL to GVL.

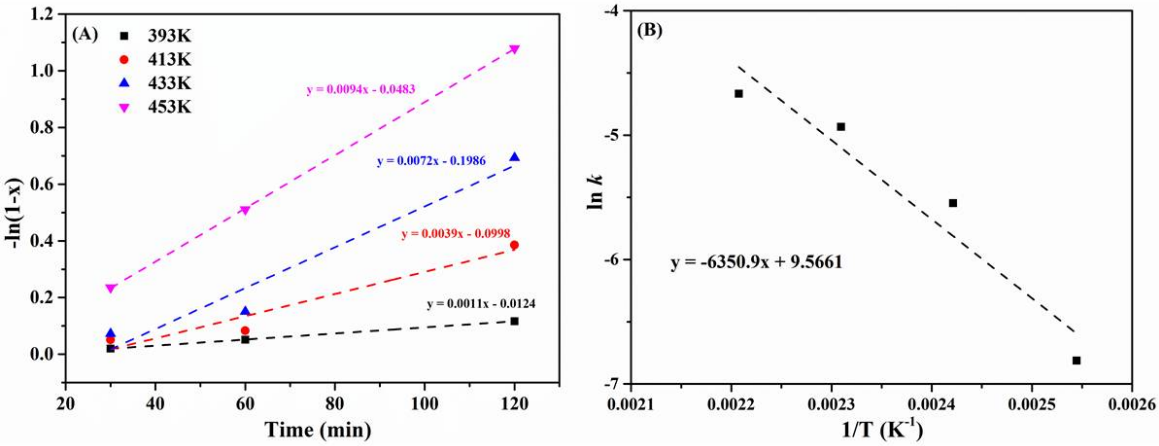

Fig. 9 (A) Kinetic profiles and (B) Arrhenius plot of PPOA-Hf-1:1.5-catalyzed conversion of EL to GVL; Reaction conditions: EL: 1 mmol, PPOA-Hf-1:1.5: 72 mg, 2-propanol: 5 mL.

3.4. Effect of Catalyst Dosage and Reactivity Comparison with Different Catalysts

In this part, the influence of catalyst dosage was examined (Fig. 10). The absence of catalyst leads to almost no GVL formed, indicating that the reaction requires the participation of the catalyst. When the catalyst dosage increased, the yield of GVL rose accordingly. At catalyst dosage of 72 mg, both GVL yield and EL conversion reach maximum. There is no further increase of GVL yield when more than 72 mg PPOA-Hf-1:1.5 was used, indicating that 72 mg (mass ratio 2:1) is the best catalyst dosage.

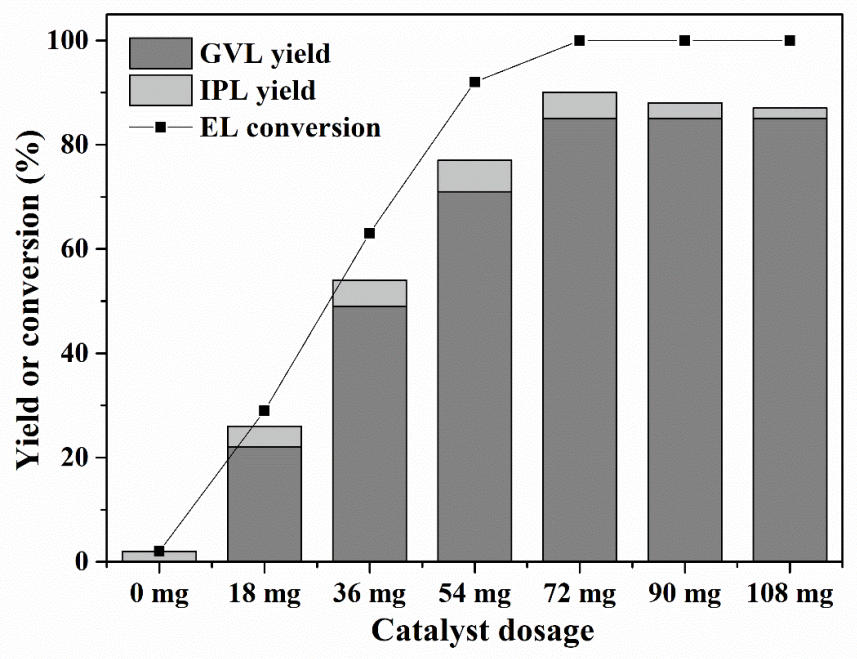

Fig. 10 Effect of catalyst dosage on conversion of EL to GVL; Reaction conditions: EL: 1 mmol, 2-propanol: 5 mL, T: 160 ºC, t: 6 h.

For comparison, several oxides and the precursor PPOA were used for the catalytic conversion of EL to GVL (Table. 1). Weak acid or base oxides such as SiO_2, TiO_2, and MgO nearly have no catalytic activity for the reaction. In contrast, amphoteric oxides including HfO_2, Al_2O_3, and ZrO_2 give GVL in a low yield of 6%, 1% and 2%, respectively. PPOA, due to its high acidity, can catalyze EL being converted to IPL (13% yield). Notably, when a strong base CaO was used, 17% yield of GVL and 43% yield of IPL were obtained. By consideration of above results, it can be deduced that base sites are helpful for GVL synthesis while may result in the formation of IPL. On the other hand, strong acid in the absence of Lewis acid species is unable to catalyze the production of GVL while may promote the cyclization or lactonization step. Due to the appropriate acid-base site content and strength, PPOA-Hf-1:1.5 can efficiently catalyze the synthesis of GVL (85% yield) from EL, which is much higher than other tested catalysts.

Table 1. Activity comparison of different solid catalysts in conversion EL to GVL [a]

Entry	Catalyst	GVL yield (%)	IPL yield (%)	EL conv. (%)	Average rate (μmol $g^{-1}h^{-1}$)[b]
1	SiO_2	<1	<1	1	<20
2	TiO_2	<1	<1	1	<20
3	MgO	<1	<1	1	<20
4	HfO_2	6	1	10	140
5	Al_2O_3	1	5	8	23
6	ZrO_2	2	-	5	46
7	PPOA	0	13	16	-
8	CaO	17	43	81	400
9	PPOA-Hf-1:1.5	85	5	100	1970

[a] Reaction conditions: EL: 1 mmol, cat: 72 mg, 2-propanol: 5 mL, T= 160 ºC t=6 h

[b] Average rate is defined as (mol of formed GVL) / (catalyst weight ×time)

3.5. Catalyst Leaching Experiments and Recycling Study

Based on the results of TG analysis, the catalyst has good thermal stability. To examine the chemical stability of the solid catalyst (PPOA-Hf-1:1.5), the hot filtration experiment was carried out. In the catalytic conversion of EL to GVL, PPOA-Hf-1:1.5 was filtered out after 3 h as soon as the reaction system cooled to ca. 80 ºC. Then the GVL yield was measured per hour in the next three hours. No significant increase in GVL yield was observed (Fig. 11), and ICP analysis shows that there is almost no Hf leaching (<0.01 ppm Hf detected). This result demonstrates that PPOA-Hf-1:1.5 is a heterogeneous catalyst, and chemically stable in the reaction system.

Furthermore, the reusability of the solid catalyst was investigated (Fig. 12), and the PPOA-Hf catalyst could be reused for five consecutive times without a significant reduction in GVL yield and EL conversion. The IR spectra in Fig.7 show that the reused

catalyst keeps the intact structure after recycling for five times. In addition, the acid and base activity sites were remained in the reused catalyst, as illustrated by NH_3- and CO_2-TPD (Fig. 4). These results prove the good reusability of the solid catalyst PPOA-Hf.

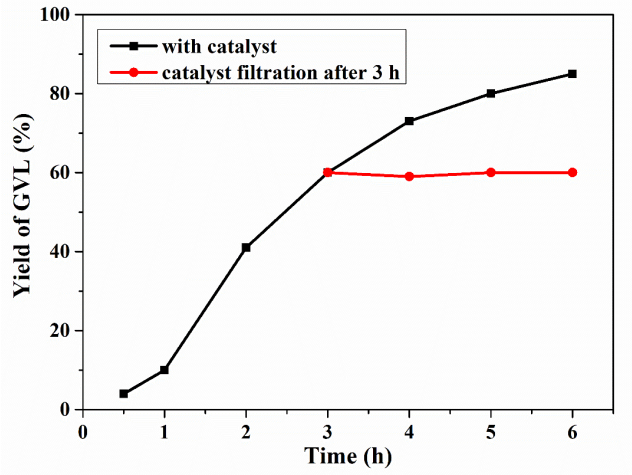

Fig. 11 Hot filtration experimental results of PPOA-Hf-1:1.5-catalyzed conversion of EL to GVL; Reaction conditions: EL: 1 mmol, PPOA-Hf-1:1.5: 72 mg, 2-propanol: 5 mL, T: 160 ℃.

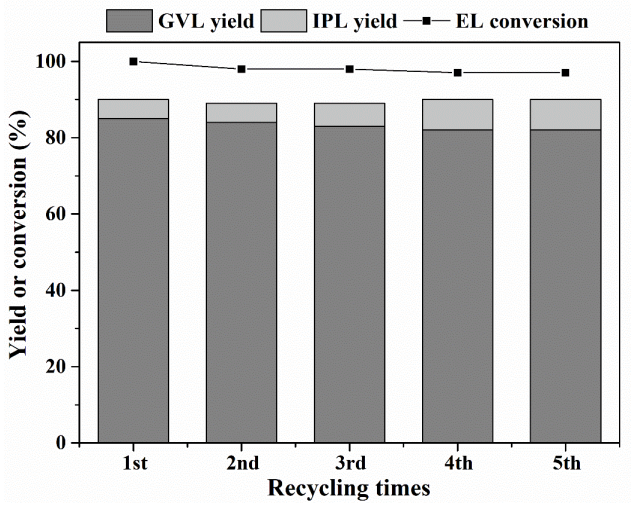

Fig. 12 Reusability of PPOA-Hf-1:1.5 in catalytic conversion of EL to GVL; Reaction conditions: EL: 1 mmol, PPOA-Hf-1:1.5: 72 mg, 2-propanol: 5 mL, T: 160 ℃, t: 6 h.

4. Conclusion

In summary, a stable Hf-containing acid-base bifunctional solid catalyst was prepared, and highly efficient for catalytic conversion of EL to GVL. A high GVL yield of 85% was obtained at 160 ºC after 6 h, which is superior to other tested catalysts. In addition, this solid catalyst PPOA-Hf-1.5 had good reusability and could be reused for 5 times without obvious activity decline.

Author Contributions

W.W., H.L. and S.Y. conceived and designed the experiments; W.W., Y.L. and W.Z. performed the experiments; W.W. and H.L. analyzed the data; W.W., H.L. and S.Y. co-wrote the paper.

Acknowledgements

This study was financially supported by the National Natural Science Foundation of China (21576059 & 21666008), Fok Ying-Tong Education Foundation (161030), Guizhou Science & Technology Foundation ([2018]1037 & [2017]5788), and Key Technologies R&D Program of China (2014BAD23B01).

Conflicts of interest

There are no conflicts to declare.

References

[1] Xu, C.; Arancon, R.A.D.; Labidi, J.; Luque, R. Lignin depolymerisation strategies: towards valuable chemicals and fuels. *Chem. Soc. Rev.* **2014**, *43*, 7485-7500. DOI: 10.1039/C4CS00235K

[2] Li, H.; Saravanamurugan, S.; Yang, S.; Riisager, A. Direct transformation of carbohydrates to the biofuel 5-ethoxymethylfurfural by solid acid catalysts. *Green Chem.* **2016**, *18*, 726-734. DOI: 10.1039/C5GC01043H

[3] Li, H.; Bhadury, P.S.; Riisager, A.; Yang, S. One-pot transformation of polysaccharides via multi-catalytic processes. *Catal. Sci. Techol.* **2014**, *4*, 4138-4168. DOI: 10.1039/C4CY00711E

[4] Holm, M.S.; Saravanamurugan, S.; Taarning, E. Conversion of sugars to lactic acid derivatives using heterogeneous zeotype catalysts. *Science* **2010**, *328*, 602-605. DOI: 10.1126/science.1183990

[5] Li, H.; Zhao, W.; Fang, Z. Hydrophobic Pd nanocatalysts for one-pot and high-yield production of liquid furanic biofuels at low temperatures. *Appl. Catal. B* **2017**, *215*, 18-27. DOI: 10.1016/j.apcatb.2017.05.039

[6] Alonso, D.M.; Wettstein, S.G.; Dumesic, J.A. Bimetallic catalysts for upgrading of biomass to fuels and chemicals. *Chem. Soc. Rev.* **2012**, *41*, 8075-8098. DOI: 10.1039/C2CS35188A

[7] Corma, A.; Iborra, S.; Velty, A. Chemical routes for the transformation of biomass into chemicals. *Chem. Rev.* **2007**, *107*, 2411-2502. DOI: 10.1021/cr050989d

[8] Liguori, F.; Moreno-Marrodan, C.; Barbaro, P. Environmentally friendly synthesis of γ-valerolactone by direct catalytic conversion of renewable rources. *ACS Catal.* **2015**, *5*, 1882-1894. DOI: 10.1021/cs501922e

[9] Li, H.; Yang, S.; Riisager, A.; Pandey, A.; Sangwan, R. S.; Saravanamurugan, S.; Luque, R. Zeolite and zeotype-catalysed transformations of biofuranic compounds. *Green Chem.* **2016**, *18*, 5701-5735. DOI: 10.1039/C6GC02415G

[10] Zhang, Z. Synthesis of γ-valerolactone from carbohydrates and its applications. *ChemSusChem* **2016**, *9*, 156-171. DOI: 10.1002/cssc.201501089

[11] Qi, X.; Guo, H.; Li, L. Y.; Smith, Jr., R.L. Acid-catalyzed dehydration of fructose into 5-hydroxymethylfurfural by cellulose-derived amorphous carbon. *ChemSusChem* **2012**, *5*, 2411-2502. DOI: 10.1002/cssc.201200363

[12] Zhou, P.; Zhang, Z. One-pot catalytic conversion of carbohydrates into furfural and 5-hydroxymethylfurfural. *Catal. Sci. Technol.* **2016**, *6*, 3694-3712. DOI: 10.1039/c6cy00384b

[13] Guo, H.; Duereh, A.; Hiraga, Y.; Aida, T.M.; Qi, X.; Smith Jr., R.L. Perfect recycle and mechanistic role of hydrogen sulfate ionic liquids as additive in ethanol for efficient conversion of carbohydrates into 5-ethoxymethylfurfural. *Chem. Eng. J.* **2017**, *323*, 287-294. DOI: 10.1016/j.cej.2017.04.111

[14] Guo, H.; Qi, X.; Hiraga, Y.; Aida, T.M.; Smith Jr., R.L. Efficient conversion of fructose into 5-ethoxymethylfurfural with hydrogen sulfate ionic liquids as co-solvent and catalyst. *Chem. Eng. J.* **2017**, *314*, 508-514. DOI: 10.1016/j.cej.2016.12.008

[15] Saravanamurugan, S.; Van Buu, O.N.; Riisager, A. Conversion of mono- and disaccharides to ethyl levulinate and ethyl pyranoside with sulfonic acid-functionalized ionic liquids. *ChemSusChem* **2011**, *4*, 723-726. DOI: 10.1002/cssc.201100137

[16] Saravanamurugan, S.; Riisager, A. Solid acid catalysed formation of ethyl levulinate and ethyl glucopyranoside from mono- and disaccharides. *Catal. Commun.* **2012**, *17*, 71-75. DOI: 10.1016/j.catcom.2011.10.001

[17] Isikgor, F.H.; Becer, C.R. Lignocellulosic biomass: a sustainable platform for the production of bio-based chemicals and polymers. *Polym. Chem.* **2015**, *6*, 4497-4559. DOI: 10.1039/C5PY00263J

[18] Saravanamurugan, S.; Riisager, A. Zeolite catalyzed transformation of carbohydrates to alkyl levulinates. *ChemCatChem* **2013**, *5*, 1754-1757. DOI: 10.1002/cctc.201300006

[19] Gilkey, M.J.; Xu, B. Heterogeneous catalytic transfer hydrogenation as an effective pathway in biomass upgrading. *ACS Catal.* **2016**, *6*, 1420-1436. DOI: 10.1021/acscatal.5b02171

[20] Li, J.; Liu, J.; Zhou, H.; Fu, Y. Catalytic transfer hydrogenation of furfural to furfuryl alcohol over nitrogen-doped carbon-supported iron catalysts. *ChemSusChem* **2016**, *9*, 1339-1347. DOI: 10.1002/cssc.201600089

[21] Wang, D.; Astruc, D. The golden age of transfer hydrogenation. *Chem. Rev.* **2015**, *115*, 6621-6686. DOI: 10.1021/acs.chemrev.5b00203

[22] Grasemann M.; Laurenczy, G. Formic acid as a hydrogen source–recent developments and future trends. *Energy Environ. Sci.* **2012**, *5*, 8171-8181. DOI: 10.1039/C2EE21928J

[23] Bigler, R.; Huber, R.; Stöckli, M.; Mezzetti, A. Iron(II)/$(NH)_2P_2$ macrocycles: modular, highly enantioselective transfer hydrogenation catalysts. *ACS Catal.* **2016**, *6*, 6455-6464. DOI: 10.1021/acscatal.6b01872

[24] Li, H.; He, J.; Riisager, A.; Saravanamurugan, S.; Song, B.; Yang, S. Acid-base bifunctional zirconium N-alkyltriphosphate nanohybrid for hydrogen transfer of Biomass-Derived Carboxides. *ACS Catal.* **2016**, *6*, 7722-7727. DOI: 10.1021/acscatal.6b02431

[25] Wang, J.; Okumura, K.; Jaenicke, S.; Chuah, G.K. Post-synthesized zirconium-containing Beta zeolite in Meerwein-Ponndorf-Verley reduction: Pros and cons. *Appl. Catal. A* **2015**, *493*, 112-120. DOI: 10.1016/j.apcata.2015.01.001

[26] Assary, R.S.; Curtiss, L.A.; Dumesic, J.A. Exploring Meerwein-Ponndorf-Verley reduction chemistry for biomass catalysis using a first-principles approach. *ACS Catal.* **2013**, *3*, 2694-2704. DOI: 10.1021/cs400479m

[27] Chia, M.; Dumesic, J.A.; Liquid-phase catalytic transfer hydrogenation and cyclization of levulinic acid and its esters to γ-valerolactone over metal oxide catalysts. *Chem. Commun.* **2011**, *47*, 12233-12235. DOI: 10.1039/C1CC14748J

[28] Tang, X.; Hu, L.; Sun, Y.; Zhao, G.; Hao, W.; Lin, L. Conversion of biomass-derived ethyl levulinate into γ-valerolactone via hydrogen transfer from supercritical ethanol over a ZrO_2 catalyst. *RSC Adv.* **2013**, *3*, 10277-10284. DOI: 10.1039/C3RA41288A

[29] Tang, X.; Chen, H.; Hu, L.; Hao, W.; Sun, Y.; Zeng, X.; Lin, L.; Liu, S.; Conversion of biomass to γ-valerolactone by catalytic transfer hydrogenation of ethyl levulinate over metal hydroxides. *Appl. Catal. B* **2014**, *147*, 827-834. DOI: 10.1016/j.apcatb.2013.10.021

[30] Li, H.; Fang, Z.; Yang, S. Direct Conversion of sugars and ethyl levulinate into γ-valerolactone with superparamagnetic acid-base bifunctional $ZrFeO_x$ nanocatalysts. *ACS Sustain. Chem. Eng*. **2016**, *4*, 236-246. DOI: 10.1021/acssuschemeng.5b01480

[31] He, J.; Li, H.; Lu, Y.; Liu, Y.; Wu, Z.; Hu, D.; Yang, S. Cascade catalytic transfer hydrogenation-cyclization of ethyl levulinate to γ-valerolactone with Al-Zr mixed oxides. *Appl. Catal. A* **2016**, *510*, 11-19. DOI: 10.1016/j.apcata.2015.10.049

[32] He, J.; Li, H.; Liu, Y.; Zhao, W.; Yang, T.; Xue, W.; Yang, S. Catalytic transfer hydrogenation of ethyl levulinate into γ-valerolactone over mesoporous Zr/B mixed oxides. *J. Ind. Eng. Chem.* **2016**, *43*, 133-141. DOI: 10.1016/j.jiec.2016.07.059

[33] Tang, X.; Zeng, X.; Li, Z.; Li, W.; Jiang, Y.; Hu, L.; Liu, S.; Sun, Y.; Lin, L. In situ generated catalyst system to convert biomass-derived levulinic acid to γ-valerolactone. *ChemCatChem* **2015**, *7*, 1372-1379. DOI: 10.1002/cctc.201500115

[34] Kuwahara, Y.; Kaburagi, W.; Osada, Y.; Fujitani, T.; Yamashita, H.; Catalytic transfer hydrogenation of biomass-derived levulinic acid and its esters to γ-valerolactone over ZrO_2 catalyst supported on SBA-15 silica. *Catal. Today* **2017**, 281, 418-428. DOI: 10.1016/j.cattod.2016.05.016

[35] de los Reyes, M.; Majewski, P.J.; Scales, N.; Luca, V. Hydrolytic stability of mesoporous zirconium titanate frameworks containing coordinating organic functionalities. *ACS Appl. Mater. Inter.* **2013**, *5*, 4120-4128. DOI: 10.1021/am3031695

[36] Li, H.; Yang, T.; Fang, Z. Biomass-derived mesoporous Hf-containing hybrid for efficient Meerwein-Ponndorf-Verley reduction at low temperatures. *Appl. Catal. B* **2018**, *227*, 79-89. DOI: 10.1016/j.apcatb.2018.01.017

[37] Gelman, F.; Blum, J.; Avnir, D. Acids and bases in one pot while avoiding their mutual destruction. *Angew. Chem.* **2001**, *113*, 3759-3761. DOI: 10.1002/1521-3773(20011001)40:19<3647::AID-ANIE3647>3.0.CO;2-A

[38] Yang, Y.; Liu, X.; Li, X.; Zhao, J.; Bai, S.; Liu, J.; Yang, Q. A yolk-shell nanoreactor with a basic core and an acidic shell for cascade reactions. *Angew. Chem.* **2012**, *124*, 9298-9302. DOI: 10.1002/ange.201204829

[39] Margelefsky, E.L.; Zeidan, R.K.; Davis, M.E. Cooperative catalysis by silica-supported organic functional groups. *Chem. Soc. Rev.* **2008**, *37*, 1118-1126. DOI: 10.1039/B710334B

[40] Li, H.; Fang, Z.; Smith Jr., R.L.; Yang, S. Efficient valorization of biomass to biofuels with bifunctional solid catalytic materials. *Prog. Energy Combust.* **2016**, *55*, 98-194. DOI: 10.1016/j.pecs.2016.04.004

[41] Veliscek-Carolan, J.; Hanley, T.L.; Luca, V. Zirconium organophosphonates as high capacity, selective lanthanide sorbents. *Sep. Purif. Technol.* **2014**, *129*, 150-158. DOI: 10.1016/j.seppur.2014.03.028

[42] Zhu, Y.; Ma, T.; Liu, Y.; Ren, T.; Yuan, Z.; Metal phosphonate hybrid materials: from densely layered to hierarchically nanoporous structures. *Inorg. Chem. Front.* **2014**, *1*, 360-383. DOI: 10.1039/C4QI00011K

[43] Ma, T.; Yuan, Z. Metal phosphonate hybrid mesostructures: environmentally friendly multifunctional materials for clean energy and other applications. *ChemSusChem* **2011**, *4*, 1407-1419. DOI: 10.1002/cssc.201100050

[44] Bhanja, P.; Bhaumik, A. Organic-inorganic hybrid metal phosphonates as recyclable heterogeneous catalysts. *ChemCatChem* **2016**, *8*, 1607-1616. DOI: 10.1002/cctc.201501303

[45] Silbernagel, R.; Martin, C.H.; Clearfield, A. Zirconium (IV) phosphonate-phosphates as efficient ion-exchange materials. *Inorg. Chem.* **2016**, *55*, 1651-1656. DOI: 10.1021/acs.inorgchem.5b02555

[46] Li, H.; Liu, X.; Yang, T.; Zhao, W.; Saravanamurugan, S.; Yang, S. Porous Zirconium-Furandicarboxylate Microspheres for Efficient Redox Conversion of Biofuranics. *ChemSusChem* **2017**, *10*, 1761-1770. DOI: 10.1002/cssc.201601898

[47] Assary, R.J.; Curtiss, L.A. Theoretical studies for the formation of γ-valero-lactone from levulinic acid and formic acid by homogeneous catalysis. *Chem. Phys. Lett.* **2012**, *541*, 21-26. DOI: 10.1016/j.cplett.2012.05.060

[48] Chalid, M.; Broekhuis, A.A.; Heeres, H.J. Experimental and kinetic modeling studies on the biphasic hydrogenation of levulinic acid to γ-valerolactone using a homogeneous water-soluble Ru-(TPPTS) catalyst. *J. Mol. Catal. A* **2011**, *341*, 14-21.

[49] Luo, H.; Consoli, D.F.; Gunther, W.R.; Román-Leshkov, Y. Investigation of the reaction kinetics of isolated Lewis acid sites in Beta zeolites for the Meerwein-Ponndorf-Verley reduction of methyl levulinate to γ-valerolactone. *J. Catal.* **2014**, *320*, 198-207. DOI: 10.1016/j.jcat.2014.10.010